Gain without population inversion in a yoked superfluorescence scheme

Luqi Yuan and Anatoly A. Svidzinsky
Texas A&M University, College Station, Texas 77843, USA and Princeton University, Princeton, New Jersey 08544, USA
(Received 23 August 2011; published 29 March 2012)

We consider a medium composed of three-level (cascade scheme) atoms prepared with coherence between the upper and the ground states (a yoked superfluorescence system). We obtain an analytical solution for propagation of seed pulses which are resonant with the upper and lower transitions for arbitrary level populations and pulse shapes. We find that if the initial coherence is large enough and the intermediate level is populated the system can have gain without population inversion. Coherence can also yield gain suppression in the inverted medium. We obtain conditions for the gain in terms of level populations and coherence.

DOI: 10.1103/PhysRevA.85.033836 PACS number(s): 42.50.Nn, 42.50.Ct

I. INTRODUCTION

Superradiance (the speedup of spontaneous emission) of atomic ensembles is a collective phenomenon which still offers interesting directions for exploration [1]. It was first predicted by Dicke in 1954 [2]. Later on it was observed by Feld and coworkers in HF gas [3]; they also gave a theoretical explanation of how an initially inverted two-level system evolves into a superradiant state [4,5]. The influence of virtual transitions on collective emission and nonlocal (retardation) effects are among the intriguing subjects of current theoretical [6–10] and experimental [11] investigation. The cooperative effects of spontaneous emission can be used for optical quantum-state storage, quantum cryptography [12], and quantum information [13].

Superfluorescence is another collective process in which the superradiant state is developed in a system of initially uncorrelated excited atoms [14]. This process starts with normal spontaneous emission but later develops correlations between the atoms [15]. In the past half century, both types of phenomena, superradiance and superfluorescence, have been extensively studied theoretically and experimentally.

The presence of quantum coherence yields interesting effects. In particular, it can lead to superfluorescence without inversion [16–20]. In such systems coherence created by a driving field on one transition influences superfluorescence on another transition. Quantum coherence can also yield lasing without inversion [21–23] which has been extensively studied during the last two decades [24–27].

Yoked superfluorescence [28] is another example of the manifestation of quantum coherence. It occurs in a three-level cascade system initially prepared with coherence between the upper and the ground states. Such coherence can be produced by a laser pump pulse propagating through the medium (the direction with the pump we call "forward" and against the pump "backward"). The laser pulse can excite the upper level from the ground state, e.g., by a two-photon process which creates some initial population in the upper level. Since the intermediate level is initially empty there is population inversion between the upper and the intermediate levels, which triggers superfluorescence in this transition. Both experimental and theoretical studies show suppression of the gain in the forward direction [29–31] at early times, when there is no population in the intermediate level, i.e., there is population inversion between the upper two levels but no population inversion between the lower two. As soon as the intermediate level becomes populated it decays into the ground state, emitting photons mainly in the forward direction [28,32,33].

Recently, the generation of backward lasing in air has been demonstrated in the experiment of Dogariu *et al*. [34]. In this experiment, the oxygen molecule O_2 is dissociated into two atoms by a strong 226 nm picosecond laser pulse focused into a 1-mm-long segment. The pulse also excites the oxygen atom from the ground $2p\,^3P$ state to the upper $3p\,^3P$ state by two-photon absorption, which prepares a 1-mm-long gain medium. Backward 845 nm lasing action was observed between the upper state and the intermediate $3s\,^3S$ state. Subsequently Traverso *et al*. showed in an experiment that when a strong nanosecond (instead of picosecond) laser pulse is used, emission becomes spiky which can be due to effects of coherence [35]. In this experiment the pulse duration ($\sim$10 ns) is much longer than the characteristic superfluorescence time scale for the upper transition ($\sim$100 ps) and, thus, the intermediate $3s\,^3S$ level is being populated.

Having in mind the air laser experiment, we here consider a medium composed of three-level atoms (cascade scheme) which is prepared with arbitrary uniform population distribution. There is also initial coherence between the upper and the ground-state levels which is assumed to be generated by a strong multiphoton resonant driving field propagating in the positive (forward) z direction. Such generated coherence contains the phase factors e^{ikz}, where $k = \omega/c$ and ω is the transition frequency. We are interested in propagation of weak seed pulses through the system in the forward and backward directions. The pulses have carrier frequencies that corresponds to the energy of the upper and lower transitions. We treat the problem semiclassically and use the Maxwell-Bloch equations. In the linear approximation we obtain an exact analytical solution for the evolution of an arbitrary initial pulse propagating through the medium. The seed pulse (vacuum fluctuations) undergoes growth or decay depending on the level populations and initial coherence.

We show that for an inverted medium the presence of initial coherence can result in forward gain suppression. This result is known in the literature [29–31]. In addition, we find that coherence can yield gain in the forward direction even if there is no population inversion on both transitions. We obtain conditions for the gain in a general form in terms of level populations and coherences.

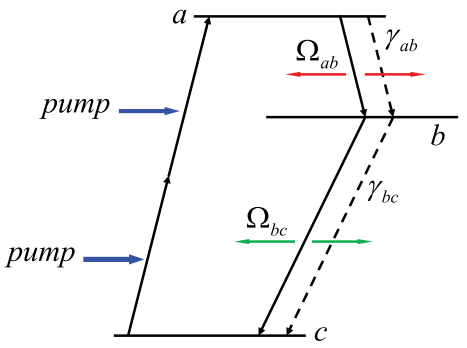

FIG. 1. (Color online) Cascade scheme of atomic energy levels.

II. EVOLUTION OF WEAK PULSES IN YOKED SUPERFLUORESCENCE SCHEME

Here we consider a medium composed of three-level atoms. Each atom is described by the cascade scheme shown in Fig. 1. The system is uniformly excited by a pump pulse multiphoton resonant with the $a \leftrightarrow c$ forbidden transition propagating along the z axis (forward direction). This process generates coherence ρ_{ac} between the upper and ground states; thus, there is correlation between atoms. Population can decay through the allowed transitions $a \to b$ and $b \to c$. We study how weak seed pulses Ω_{ab} and Ω_{bc}, having carrier frequencies corresponding to the $a \leftrightarrow b$ and $b \leftrightarrow c$ transitions, propagate through the medium. In our analytical calculations we assume that during the seed pulse propagation the level populations ρ_{aa}, ρ_{bb}, and ρ_{cc}, as well as the coherence ρ_{ac}, remain constant. However, the initial seed pulse shapes $\Omega_{ab}(0,z)$ and $\Omega_{bc}(0,z)$ are arbitrary.

We treat the problem semiclassically in the framework of the Maxwell-Bloch equations, assuming that the electric field and atomic density matrix depend only on the coordinate z and time t. The equations of motion for the atomic density matrix read

$$\dot{\rho}_{ab}(t,z) = -\Gamma_{ab}\rho_{ab}(t,z) - i\Omega_{ab}(t,z)n_{ab} - i\Omega^*_{bc}(t,z)\rho_{ac}, \quad (1)$$

$$\dot{\rho}_{bc}(t,z) = -\Gamma_{bc}\rho_{bc}(t,z) - i\Omega_{bc}(t,z)n_{bc} + i\Omega^*_{ab}(t,z)\rho_{ac}, \quad (2)$$

where $n_{ab} = \rho_{aa} - \rho_{bb}$, $n_{bc} = \rho_{bb} - \rho_{cc}$, and ρ_{ac} are constants, $\Gamma_{ij} = \Gamma + \gamma_{ij}/2$, Γ is the dephasing rate due to collisional broadening, and γ_{ij} is the spontaneous decay rate of the corresponding transition. In a more realistic system there is also Doppler broadening and dephasing due to the time of flight of the atom across the active medium. However, in experiments the atomic density is usually greater than 10^{14} cm^{-3} and, thus, the superradiant time scale is shorter than 10 ps. Hence, the line broadening due to superradiant emission is much larger than the Doppler broadening ($\sim 10^{10}$ s^{-1}) and the dephasing rate due to time of flight ($\sim 10^{8}$ s^{-1}).

The propagation equations for the electric field are

$$\frac{\partial\Omega_{ab}(t,z)}{\partial z} + \frac{1}{c}\frac{\partial\Omega_{ab}(t,z)}{\partial t} = i\eta_{ab}\rho_{ab}(t,z), \quad (3)$$

$$\frac{\partial\Omega_{bc}(t,z)}{\partial z} + \frac{1}{c}\frac{\partial\Omega_{bc}(t,z)}{\partial t} = i\eta_{bc}\rho_{bc}(t,z), \quad (4)$$

where Ω_{ij} is the Rabi frequency corresponding to the electric field envelope, $\eta_{ij} = 3N\lambda_{ij}^2\gamma_{ij}/8\pi$ is the atom-field interaction constant, N is the atomic density, and λ_{ij} is the transition wavelength. Equations (1) and (2) are written for the fields Ω_{ab} and Ω_{bc} propagating in the forward direction. For the backward-propagating fields there is no ρ_{ac} term in Eqs. (1) and (2) because in this case the phases of ρ_{ab} and ρ_{bc} cannot match the phase of the coherence ρ_{ac}. Indeed, for the backward propagation, ρ_{ab} and ρ_{bc} have the same phases as the backward fields Ω_{ab} and Ω_{bc}, that is, $ik_{ab}z$ and $ik_{bc}z$. However, the phase of the initial coherence ρ_{ac} is produced by the forward pump field and has the value $-i(k_{ab}+k_{bc})z$. Therefore, for the backward direction, the last term in Eq. (1) has the phase $-i(k_{ab}+k_{bc})z - ik_{bc}z$, which differs from the phase of ρ_{ab} by $-2i(k_{ab}+k_{bc})z$. The phase difference leads to a fast-oscillating term as a function of z. In the rotating-wave approximation such terms have to be omitted. As a result, the solution for backward propagation can be obtained from the forward solution by taking $\rho_{ac} = 0$.

We solve Eqs. (1)–(4) with the initial condition $\rho_{ab}(0,z) = \rho_{bc}(0,z) = 0$ and initial pulse shapes $\Omega_{ab}(0,z)$ and $\Omega_{bc}(0,z)$. Equation (1) gives

$$\rho_{ab}(t,z) = -in_{ab}\int_0^t \Omega_{ab}(t',z)e^{-\Gamma_{ab}(t-t')}dt' - i\rho_{ac}\int_0^t \Omega^*_{bc}(t',z)e^{-\Gamma_{ab}(t-t')}dt'. \quad (5)$$

Then using Eq. (3) we obtain

$$\frac{\partial\Omega_{ab}(t,z)}{\partial z} + \frac{1}{c}\frac{\partial\Omega_{ab}(t,z)}{\partial t} = \eta_{ab}n_{ab}\int_0^t \Omega_{ab}(t',z)e^{-\Gamma_{ab}(t-t')}dt' + \eta_{ab}\rho_{ac}\int_0^t \Omega^*_{bc}(t',z)e^{-\Gamma_{ab}(t-t')}dt'. \quad (6)$$

Introduction of the Laplace transform in time,

$$\hat{\Omega}(s,z) = \mathcal{L}\{\Omega(t,z)\} = \int_0^\infty e^{-st}\Omega(t,z)dt, \quad (7)$$

yields

$$\frac{\partial\hat{\Omega}_{ab}(s,z)}{\partial z} + \frac{s}{c}\hat{\Omega}_{ab}(s,z) - \frac{1}{c}\Omega_{ab}(0,z) = \eta_{ab}n_{ab}\frac{\hat{\Omega}_{ab}(s,z)}{s+\Gamma_{ab}} + \eta_{ab}\rho_{ac}\frac{\hat{\Omega}^*_{bc}(s,z)}{s+\Gamma_{ab}}. \quad (8)$$

Similarly, for Ω_{bc} we obtain the equation

$$\frac{\partial\hat{\Omega}^*_{bc}(s,z)}{\partial z} + \frac{s}{c}\hat{\Omega}^*_{bc}(s,z) - \frac{1}{c}\Omega^*_{bc}(0,z) = \eta_{bc}n_{bc}\frac{\hat{\Omega}^*_{bc}(s,z)}{s+\Gamma_{bc}} - \eta_{bc}\rho^*_{ac}\frac{\hat{\Omega}_{ab}(s,z)}{s+\Gamma_{bc}}. \quad (9)$$

The solution of Eqs. (8) and (9) can be rewritten as

$$\hat{\Omega}_{ab}(s,z) = \frac{1}{c}\int_{-\infty}^{z} dz'\frac{F(z')}{\lambda_1-\lambda_2}[e^{\lambda_1(z-z')} - e^{\lambda_2(z-z')}], \quad (10)$$

where the source function is

$$F(z)=\frac{\eta_{ab}\rho_{ac}}{s+\Gamma_{ab}}\Omega_{bc}^{*}(0,z)+\left(\frac{s}{c}-\frac{\eta_{bc}n_{bc}}{s+\Gamma_{bc}}\right)\Omega_{ab}(0,z)+\frac{\partial\Omega_{ab}(0,z)}{\partial z} \tag{11}$$

and the constants $\lambda_{1,2}$ are

$$\lambda_{1,2}=\frac{1}{2}\left[\left(-\frac{2s}{c}+\frac{\eta_{ab}n_{ab}}{s+\Gamma_{ab}}+\frac{\eta_{bc}n_{bc}}{s+\Gamma_{bc}}\right)\pm\sqrt{\left(\frac{\eta_{ab}n_{ab}}{s+\Gamma_{ab}}-\frac{\eta_{bc}n_{bc}}{s+\Gamma_{bc}}\right)^{2}-4\frac{\eta_{ab}\rho_{ac}}{s+\Gamma_{ab}}\frac{\eta_{bc}\rho_{ac}^{*}}{s+\Gamma_{bc}}}\right]. \tag{12}$$

In the limit that the collisional dephasing Γ is much larger than the spontaneous decay rates γ_{ij} we have $\Gamma_{ab}\approx\Gamma_{bc}\approx\Gamma$, and the constants $\lambda_{1,2}$ reduce to

$$\lambda_{1,2}=-\frac{s}{c}-\frac{\xi_{1,2}}{s+\Gamma}, \tag{13}$$

where

$$\xi_{1,2}=-\tfrac{1}{2}[\eta_{ab}n_{ab}+\eta_{bc}n_{bc}\pm\zeta], \tag{14}$$

$$\zeta=\sqrt{(\eta_{ab}n_{ab}-\eta_{bc}n_{bc})^{2}-4\eta_{ab}\eta_{bc}|\rho_{ac}|^{2}}. \tag{15}$$

In this limit the inverse Laplace transform of Eq. (10) yields the following final answer for pulse evolution in the forward direction:

$$\begin{aligned}\Omega_{ab}(t,z)=\Omega_{ab}(0,z-ct)+\int_{z-ct}^{z}dz'\Omega_{ab}(0,z')e^{-(\Gamma/c)(z'+ct-z)}\left\{\frac{\xi_1+\eta_{bc}n_{bc}}{\zeta}\sqrt{\frac{\xi_1(z-z')/c}{z'+ct-z}}J_1\left[2\sqrt{\frac{\xi_1}{c}(z-z')(z'+ct-z)}\right]\right.\\ \left.-\frac{\xi_2+\eta_{bc}n_{bc}}{\zeta}\sqrt{\frac{\xi_2(z-z')/c}{z'+ct-z}}J_1\left[2\sqrt{\frac{\xi_2}{c}(z-z')(z'+ct-z)}\right]\right\}-\int_{z-ct}^{z}dz'\frac{\eta_{ab}\rho_{ac}}{\zeta}\Omega_{bc}^{*}(0,z')e^{-(\Gamma/c)(z'+ct-z)}\\ \times\left\{\sqrt{\frac{\xi_1(z-z')/c}{z'+ct-z}}J_1\left[2\sqrt{\frac{\xi_1}{c}(z-z')(z'+ct-z)}\right]-\sqrt{\frac{\xi_2(z-z')/c}{z'+ct-z}}J_1\left[2\sqrt{\frac{\xi_2}{c}(z-z')(z'+ct-z)}\right]\right\},\end{aligned} \tag{16}$$

where $\xi_{1,2}$ and ζ are defined in Eqs. (14) and (15), and $J_1(z)$ is the Bessel function. Similarly, the solution for the field Ω_{bc} reads

$$\begin{aligned}\Omega_{bc}^{*}(t,z)=\Omega_{bc}^{*}(0,z-ct)+\int_{z-ct}^{z}dz'\Omega_{bc}^{*}(0,z')e^{-(\Gamma/c)(z'+ct-z)}\left\{\frac{\xi_1+\eta_{ab}n_{ab}}{\zeta}\sqrt{\frac{\xi_1(z-z')/c}{z'+ct-z}}J_1\left[2\sqrt{\frac{\xi_1}{c}(z-z')(z'+ct-z)}\right]\right.\\ \left.-\frac{\xi_2+\eta_{ab}n_{ab}}{\zeta}\sqrt{\frac{\xi_2(z-z')/c}{z'+ct-z}}J_1\left[2\sqrt{\frac{\xi_2}{c}(z-z')(z'+ct-z)}\right]\right\}+\int_{z-ct}^{z}dz'\frac{\eta_{bc}\rho_{ac}^{*}}{\zeta}\Omega_{ab}(0,z')e^{-(\Gamma/c)(z'+ct-z)}\\ \times\left\{\sqrt{\frac{\xi_1(z-z')/c}{z'+ct-z}}J_1\left[2\sqrt{\frac{\xi_1}{c}(z-z')(z'+ct-z)}\right]-\sqrt{\frac{\xi_2(z-z')/c}{z'+ct-z}}J_1\left[2\sqrt{\frac{\xi_2}{c}(z-z')(z'+ct-z)}\right]\right\}.\end{aligned} \tag{17}$$

To obtain the evolution of the backward pulse we set $\rho_{ac}=0$ in the above equations and find

$$\Omega_{ab}(t,z)=\Omega_{ab}(0,z-ct)+\sqrt{\frac{\eta_{ab}n_{ab}}{c}}\int_{z-ct}^{z}dz'\Omega_{ab}(0,z')e^{-(\Gamma/c)(z'+ct-z)}\sqrt{\frac{z-z'}{z'+ct-z}}I_1\left[2\sqrt{\frac{\eta_{ab}n_{ab}}{c}}\sqrt{(z-z')(z'+ct-z)}\right], \tag{18}$$

$$\Omega_{bc}(t,z)=\Omega_{bc}(0,z-ct)+\sqrt{\frac{\eta_{bc}n_{bc}}{c}}\int_{z-ct}^{z}dz'\Omega_{bc}(0,z')e^{-(\Gamma/c)(z'+ct-z)}\sqrt{\frac{z-z'}{z'+ct-z}}I_1\left[2\sqrt{\frac{\eta_{bc}n_{bc}}{c}}\sqrt{(z-z')(z'+ct-z)}\right], \tag{19}$$

where $I_1(z)$ is the modified Bessel function.

Equations (16)–(19) give the exact analytical answer as to how the initial weak pulses $\Omega_{ab}(0,z)$ and $\Omega_{bc}(0,z)$ propagate through the medium. As an illustration, we consider a simple example of a δ-function initial pulse $\Omega_{ab}(0,z)=\Omega_{ab}^{(0)}\delta(z)$ and no initial pulse at the $b\leftrightarrow c$ transition $\Omega_{bc}(0,z)=0$. Then Eqs. (16) and (17) yield for the forward direction

$$\begin{aligned}\Omega_{ab}(t,z)=\Omega_{ab}^{(0)}\delta(z-ct)+\Omega_{ab}^{(0)}e^{-\Gamma(t-z/c)}\left\{\frac{\xi_1+\eta_{bc}n_{bc}}{\zeta}\sqrt{\frac{\xi_1 z/c}{ct-z}}J_1\left[2\sqrt{\frac{\xi_1}{c}z(ct-z)}\right]\right.\\ \left.-\frac{\xi_2+\eta_{bc}n_{bc}}{\zeta}\sqrt{\frac{\xi_{-}z/c}{ct-z}}J_1\left[2\sqrt{\frac{\xi_2}{c}z(ct-z)}\right]\right\}\theta(ct-z),\end{aligned} \tag{20}$$

$$\Omega^*_{bc}(t,z) = \frac{\eta_{bc}\rho^*_{ac}}{\zeta}\Omega^{(0)}_{ab}e^{-\Gamma(t-z/c)}\left\{\sqrt{\frac{\xi_1 z/c}{ct-z}}J_1\left[2\sqrt{\frac{\xi_1}{c}z(ct-z)}\right] - \sqrt{\frac{\xi_2 z/c}{ct-z}}J_1\left[2\sqrt{\frac{\xi_2}{c}z(ct-z)}\right]\right\}\theta(ct-z). \quad (21)$$

For the backward direction we obtain

$$\Omega_{ab}(t,z) = \Omega^{(0)}_{ab}\delta(z-ct) + \sqrt{\frac{\eta_{ab}n_{ab}}{c}}\Omega^{(0)}_{ab}e^{-(\Gamma/c)(ct-z)}\sqrt{\frac{z}{ct-z}}I_1\left[2\sqrt{\frac{\eta_{ab}n_{ab}}{c}}\sqrt{z(ct-z)}\right]\theta(ct-z), \quad (22)$$

$$\Omega_{bc}(t,z) = 0. \quad (23)$$

The first term in Eqs. (20) and (22) corresponds to the initial seed pulse propagating in free space. The other terms are coming from the interaction between the atoms and the electric field.

III. FORWARD GAIN SUPPRESSION AND FORWARD GAIN WITHOUT POPULATION INVERSION

We assume that the atomic sample is $L = 1$ cm long, so it takes 0.033 ns for the photon to travel through the system. The density of atoms is large enough that the coupling constants are $\eta = \eta_{ab} = \eta_{bc} = 1000\ \text{cm}^{-1}\ \text{ns}^{-1}$. We take the dephasing rate $\Gamma = 1\ \text{ns}^{-1}$. The pulse evolution is mainly governed by collective (superradiant) effects and occurs on a time scale much faster than the dephasing time. Thus the assumption of a constant ρ_{ac} is valid.

In Fig. 2 we plot the output fields $\Omega_{ab}(t,z)$ and $\Omega_{bc}(t,z)$ given by Eqs. (20)–(22) at the edge of the sample $z = L$ as a function of time. We assume the following population distribution: $\rho_{aa} = 0.2$, $\rho_{bb} = 0.05$, $\rho_{cc} = 0.75$, and coherence $\rho_{ac} = \sqrt{0.15}i$. Both forward and backward fields at the $a \to b$ transition are shown. Please note that in the plot we do not show the δ-function term in Eqs. (20) and (22).

Emission in the backward direction grows exponentially with time as expected for an inverted medium (in the present example there is population inversion between levels a and b). According to Eq. (22) it is asymptotic to the modified Bessel function. However, the forward emission is affected by the coherence ρ_{ac}. The presence of such coherence makes the forward field oscillate and decay at long times. This behavior indicates a forward gain suppression which was previously reported in the literature [28,29]. The forward field on the $b \to c$ transition shows similar features. In the present example we do not include the backward field on the $b \to c$ transition [36].

Next we take the population distribution $\rho_{aa} = 0.1$, $\rho_{bb} = 0.3$, $\rho_{cc} = 0.6$, and coherence $\rho_{ac} = \sqrt{0.06}i$. Now there is no population inversion in either transition. The output fields $\Omega_{ab}(t,z)$ and $\Omega_{bc}(t,z)$ at the edge of the sample are shown in Fig. 3. In the present example the backward field at the $a \to b$ transition decays because there is no population inversion. Namely, for $n_{ab} < 0$ Eq. (22) yields

$$\Omega_{ab}(t,z) = \Omega^{(0)}_{ab}\delta(z-ct) - \sqrt{\frac{\eta_{ab}|n_{ab}|}{c}}\Omega^{(0)}_{ab}e^{-(\Gamma/c)(ct-z)} \times \sqrt{\frac{z}{ct-z}}J_1\left[2\sqrt{\frac{\eta_{ab}|n_{ab}|}{c}}\sqrt{z(ct-z)}\right]\theta(ct-z), \quad (24)$$

that is, the pulse decays according to the asymptote of the Bessel function J_1. However, the coherence ρ_{ac} yields enhancement of both forward fields $\Omega_{ab}(t,z)$ and $\Omega_{bc}(t,z)$. Thus, there is forward gain without population inversion in our system.

In addition to our analytical results we solved the full Maxwell-Bloch equations numerically including population

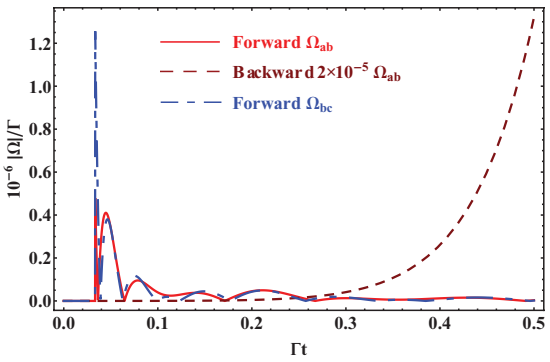

FIG. 2. (Color online) Output fields at the edge of the sample as a function of time given by Eqs. (20)–(22) with population distribution $\rho_{aa} = 0.2$, $\rho_{bb} = 0.05$, $\rho_{cc} = 0.75$, and coherence $\rho_{ac} = \sqrt{0.15}i$. The solid line shows the output forward field at the $a \to b$ transition, the dashed line is the output backward field at the $a \to b$ transition divided by 5×10^4, while the dash-dotted line is the forward field at the $b \to c$ transition.

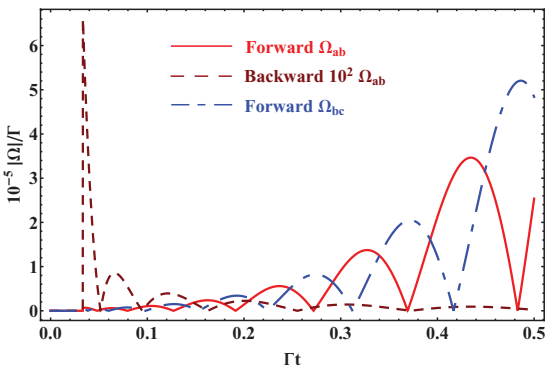

FIG. 3. (Color online) Output fields at the edge of the sample as a function of time given by Eqs. (20)–(22) with population distribution $\rho_{aa} = 0.1$, $\rho_{bb} = 0.3$, $\rho_{cc} = 0.6$, and coherence $\rho_{ac} = \sqrt{0.06}i$. The solid line shows the output forward field at the $a \to b$ transition, the dashed line is the output backward field at the $a \to b$ transition multiplied by 100, while the dash-dotted line is the forward field at the $b \to c$ transition.

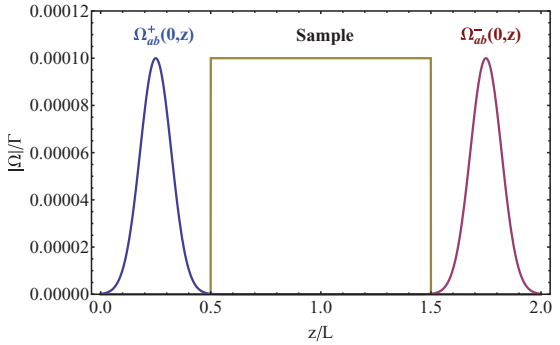

FIG. 4. (Color online) Gaussian-shaped initial seed pulses for the forward and backward fields used in numerical simulations.

dynamics and pulse propagation in both forward and backward directions. In numerical simulations, instead of δ-function pulses, Gaussian-shaped pulses are used for the initial seed for the forward and backward fields at the $a \to b$ transition (see Fig. 4). The full width at half maximum of the seed pulse is taken as $\Delta z = 0.167L$. The results of simulations are shown in Fig. 5. The numerical solution exhibits similar features to the analytical result with the δ-function seed. When there is population inversion between levels a and b, the numerical simulations show forward gain suppression in the $a \to b$ transition [see Fig. 5(a)], while with no population inversion there is forward gain [see Fig. 5(b)].

To show that lasing would also occur starting from atomic fluctuations, we calculated numerically the forward and backward emission using quantum noise as a seed instead of sending seed pulses. We found that if there is gain in the medium then simulations with the seed pulses and noise give very similar results. Thus, our analysis based on seed pulse propagation adequately describes the system's evolution.

IV. CONDITIONS FOR GAIN IN THE FORWARD DIRECTION

The analytical results we obtained allow us to find the conditions for positive gain in the forward direction. If we disregard the dephasing Γ, the gain is positive if ζ in Eq. (15) is imaginary, which yields the condition

$$4\eta_{ab}\eta_{bc}|\rho_{ac}|^2 > (\eta_{ab}n_{ab} - \eta_{bc}n_{bc})^2. \tag{25}$$

The gain is also positive if ξ_1 or ξ_2 has a negative real part, that is,

$$\eta_{ab}n_{ab} + \eta_{bc}n_{bc} + \sqrt{(\eta_{ab}n_{ab} - \eta_{bc}n_{bc})^2 - 4\eta_{ab}\eta_{bc}|\rho_{ac}|^2} > 0. \tag{26}$$

If $\eta_{ab} = \eta_{bc}$ then conditions (25) and (26) reduce to

$$2|\rho_{ac}| > |n_{ab} - n_{bc}| = |1 - 3\rho_{bb}|, \tag{27}$$

$$\rho_{aa} - \rho_{cc} + \sqrt{(1 - 3\rho_{bb})^2 - 4|\rho_{ac}|^2} > 0. \tag{28}$$

If one of the inequalities (27) and (28) is satisfied then there is positive gain in the forward direction. If $\rho_{ac} = 0$ then Eq. (28) yields the requirement that $\rho_{aa} > \rho_{bb}$. If we increase $|\rho_{ac}|$ then condition (28) may no longer be satisfied even if there is population inversion between levels a and b. This yields forward gain suppression due to coherence. However, if $|\rho_{ac}|$ is large enough and level b is populated ($\rho_{bb} \neq 0$) then one can fulfill inequality (27) even if there is no population inversion on the $a \to b$ and $b \to c$ transitions. In this range of parameters the system has forward gain without inversion. Please note that the requirement $\rho_{bb} \neq 0$ is crucial and, thus, to observe such a regime one should wait until level b becomes populated.

The physics behind our results can be understood by noting an analogy between Eqs. (1)–(4) and the equations of motion of coupled damped harmonic oscillators. Let us consider the spatially uniform case, assuming that the medium, as well as the pulses, is infinitely long. Then, introducing the notation $\Omega_{ab} = x$ and $\Omega_{bc} = y$, we can write Eqs. (1)–(4) as

$$\ddot{x} + \Gamma_{ab}\dot{x} - c\eta_{ab}n_{ab}x - c\eta_{ab}\rho_{ac}y = 0, \tag{29}$$

$$\ddot{y} + \Gamma_{bc}\dot{y} - c\eta_{bc}n_{bc}y + c\eta_{bc}\rho_{ac}x = 0. \tag{30}$$

These equations show that the coherence ρ_{ac} provides coupling between the two oscillators. The equilibrium point $x = y = 0$ is unstable (positive gain) if the oscillator matrix

$$\begin{pmatrix} c\eta_{ab}n_{ab} & c\eta_{ab}\rho_{ac} \\ -c\eta_{bc}\rho_{ac} & c\eta_{bc}n_{bc} \end{pmatrix} \tag{31}$$

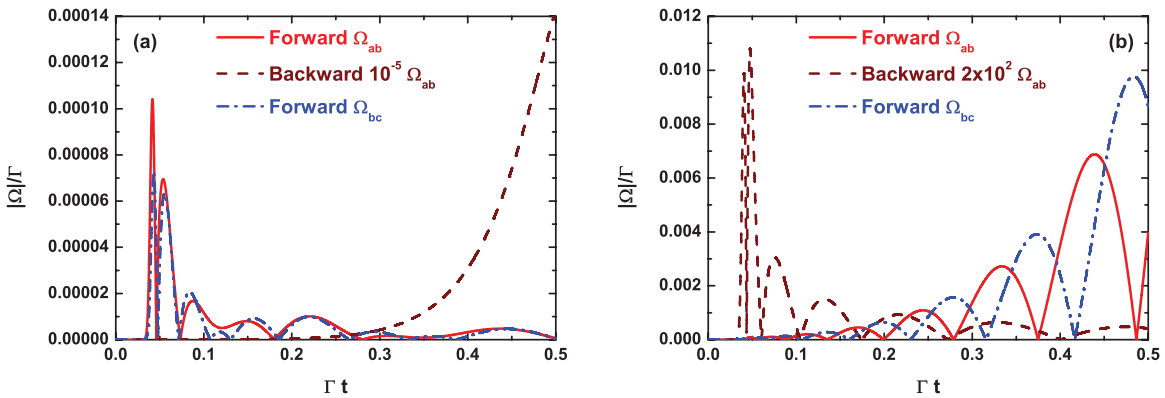

FIG. 5. (Color online) Output fields at the edge of the sample as a function of time obtained by numerical solution of the Maxwell-Bloch equations with Gaussian seed pulses and initial conditions $\rho_{aa} = 0.2$, $\rho_{bb} = 0.05$, $\rho_{cc} = 0.75$, $\rho_{ac} = \sqrt{0.15}i$ (a) and $\rho_{aa} = 0.1$, $\rho_{bb} = 0.3$, $\rho_{cc} = 0.6$, $\rho_{ac} = \sqrt{0.06}i$ (b).

has eigenvalues which are complex or have positive real part. Taking into account that the matrix eigenvalues are

$$\lambda_{1,2} = \frac{c}{2}(\eta_{ab}n_{ab} + \eta_{bc}n_{bc} \pm \sqrt{(\eta_{ab}n_{ab} - \eta_{bc}n_{bc})^2 - 4\eta_{ab}\eta_{bc}|\rho_{ac}|^2}), \quad (32)$$

we obtain conditions for the gain which coincide with Eqs. (25) and (26). So the physics behind forward gain without inversion and forward gain suppression with inversion is the same as the physics of stability of coupled harmonic oscillators.

V. CONCLUSION

In this paper, we consider pulse propagation through a medium composed of three-level (cascade scheme) atoms with initial coherence between the upper and ground states. We obtain analytical solutions for the pulse evolution for arbitrary initial populations and pulse shapes. Emission in the forward direction is similar to yoked superfluorescence, that is, there is simultaneous emission on the upper and lower transitions. We find that initial coherence can result in gain in the forward direction without inversion if the intermediate level is populated. On the other hand, coherence can suppress forward gain even in an inverted medium.

In the air laser experiment [35] it is likely that the system experiences both regimes. In this experiment, the pump pulse first partially excites the upper level a, which produces population inversion between the upper two levels. This yields backward lasing at early times, which transfers population from the upper level to the middle level b. During this process, the forward gain is suppressed. After some time, the upper-state population is depleted. This promotes the system into a state with $\rho_{aa} < \rho_{bb} < \rho_{cc}$, while the long pump pulse continues to generate coherence ρ_{ac}. For these conditions, forward gain can be achieved as we show here. These processes are repeated as long as the pump field is on.

Our work combines lasing and superradiance. In the case of a laser (with or without inversion) a weak seed pulse grows exponentially in the linear regime. In the case of superradiance in an extended medium the emitted pulse decays, undergoing oscillations with the collective frequency. The present problem combines these two effects, which yields the possibility of exponential growth and oscillations of the pulse at the same time.

ACKNOWLEDGMENTS

The authors thank Marlan O. Scully for helpful discussion. We gratefully acknowledge support for this work by National Science Foundation Grant No. EEC-0540832 (MIRTHE ERC), the Office of Naval Research, and the Robert A. Welch Foundation (Grant No. A-1261). L.Y. is supported by the Herman F. Heep and Minnie Belle Heep Texas A&M University Endowed Fund held and administered by the Texas A&M Foundation.

[1] M. O. Scully and A. A. Svidzinsky, Science **325**, 1510 (2009).
[2] R. H. Dicke, Phys. Rev. **93**, 99 (1954).
[3] N. Skribanowitz, I. P. Herman, J. C. MacGillivray, and M. S. Feld, Phys. Rev. Lett. **30**, 309 (1973).
[4] J. C. MacGillivray and M. S. Feld, Phys. Rev. A **14**, 1169 (1976).
[5] J. C. MacGillivray and M. S. Feld, Phys. Rev. A **23**, 1334 (1981).
[6] A. A. Svidzinsky, J. T. Chang, and M. O. Scully, Phys. Rev. Lett. **100**, 160504 (2008).
[7] M. O. Scully, Phys. Rev. Lett. **102**, 143601 (2009).
[8] R. Friedberg and J. T. Manassah, Phys. Lett. A **374**, 1648 (2010).
[9] A. A. Svidzinsky, J. T. Chang, and M. O. Scully, Phys. Rev. A **81**, 053821 (2010).
[10] A. A. Svidzinsky, Opt. Commun. **284**, 269 (2011); Phys. Rev. A **85**, 013821 (2012).
[11] R. Röhlsberger, K. Schlage, B. Sahoo, S. Couet, and R. Rüffer, Science **328**, 1248 (2010).
[12] A. Kalachev and S. Kröll, Phys. Rev. A **74**, 023814 (2006).
[13] D. Porras and J. I. Cirac, Phys. Rev. A **78**, 053816 (2008).
[14] R. Bonifaci and L. A. Lugiato, Phys. Rev. A **11**, 1507 (1975); **12**, 587 (1975).
[15] S. Prasad and R. J. Glauber, Phys. Rev. A **31**, 1583 (1985).
[16] V. A. Malyshev, F. Carreño, M. A. Antón, O. G. Calderón, and F. Domínguez-Adame, J. Opt. B: Quantum Semiclassical Opt. **5**, 313 (2003).
[17] V. Kozlov, O. Kocharovskaya, Y. Rostovtsev, and M. Scully, Phys. Rev. A **60**, 1598 (1999).
[18] V. A. Malyshev, I. V. Ryzhov, E. D. Trifonov, and A. I. Zaitsev, Laser Phys. **8**, 494 (1998).
[19] A. I. Zaitsev, I. V. Ryzhov, E. D. Trifonov, and V. A. Malyshev, Laser Phys. **9**, 876 (1999).
[20] A. A. Bogdanov, A. I. Zaĭtsev, and I. V. Ryzhov, Opt. Spectrosc. **89**, 1012 (2000).
[21] O. A. Kocharovskaya and Ya. I. Khanin, Zh. Eksp. Teor. Phys. **90**, 1610 (1986) [JETP **63**, 945 (1986)] Pis'ma Zh. Eksp. Teor. Fiz. **48**, 581 (1988) [JETP Lett. **48**, 630 (1988)].
[22] S. E. Harris, Phys. Rev. Lett. **62**, 1033 (1989).
[23] M. O. Scully and M. S. Zubairy, *Quantum Optics* (Cambridge University Press, Cambridge, UK, 1997).
[24] A. S. Manka, J. P. Dowling, C. M. Bowden, and M. Fleischhauer, Quantum Opt. **6**, 371 (1994).
[25] O. Kocharovskaya, Hyperfine Interact. **107**, 187 (1997).
[26] J. Mompart and R. Corbalán, J. Opt. B: Quantum Semiclassical Opt. **2**, R7 (2000).
[27] M. O. Scully and M. Fleischhauer, Science **263**, 337 (1994).
[28] J. H. Brownell, X. Lu, and S. R. Hartmann, Phys. Rev. Lett. **75**, 3265 (1995).
[29] W. R. Garrett, Phys. Rev. Lett. **70**, 4059 (1993).
[30] J. T. Manassah and I. Gladkova, Opt. Commun. **179**, 51 (2000).
[31] H. Brownell, B. Gross, X. Lu, S. R. Hartmann, and J. T. Manassah, Laser Phys. **3**, 509 (1993).

[32] D. Felinto, L. H. Acioli, and S. S. Vianna, Opt. Lett. **25**, 917 (2000).
[33] G. O. Ariunbold, M. M. Kash, V. A. Sautenkov, H. Li, Y. V. Rostovtsev, G. R. Welch, and M. O. Scully, Phys. Rev. A **82**, 043421 (2010).
[34] A. Dogariu, J. B. Michael, M. O. Scully, and R. B. Miles, Science **331**, 442 (2011).
[35] A. J. Traverso *et al*. (unpublished).
[36] The initial seed for the backward field on the $b \rightarrow c$ transition will be amplified only if there is population inversion between the lower two levels. In the present example, there is no population inversion between levels b and c, so we do not include the seed field for this transition in our plot.